Available online at www.sciencedirect.com

jmr&t Journal of Materials Research and Technology

journal homepage: www.elsevier.com/locate/jmrt

Original Article

Synthesis of clay geopolymers using olive pomace fly ash as an alternative activator. Influence of the additional commercial alkaline activator used

M.A. Gómez-Casero [a], F.J. Moral-Moral [a], L. Pérez-Villarejo [b,c], P.J. Sánchez-Soto [d], D. Eliche-Quesada [a,c,*]

[a] Department of Chemical, Environmental, and Materials Engineering, Higher Polytechnic School of Jaén, University of Jaén, Campus Las Lagunillas s/n, 23071, Jaén, Spain

[b] Department of Chemical, Environmental, and Materials Engineering, Higher Polytechnic School of Linares, University of Jaén, Campus Científico-Tecnológico, Cinturón Sur s/n, 23700, Linares (Jaén), Spain

[c] Center for Advanced Studies in Earth Sciences, Energy and Environment (CEACTEMA), University of Jaén, Campus Las Lagunillas, s/n, 23071, Jaén, Spain

[d] Institute of Materials Science of Sevilla (ICMS), Joint Center of the Spanish National Research Council (CSIC), University of Sevilla, 41092, Sevilla, Spain

ARTICLE INFO

Article history:
Received 10 January 2021
Accepted 28 March 2021
Available online 2 April 2021

Keywords:
Geopolymers
Clay
Olive pomace fly ash
Valorization
Alkaline activator
Sustainability

ABSTRACT

In this research, the use of olive pomace fly ash (OPFA) as an alkaline source for the activation of calcined clays (CC) from Bailén (Jaén, Spain) was studied. The optimal composition was obtained for 70 wt % CC and 30 wt % OPFA. The physical, mechanical and thermal properties of control geopolymers that use water as a liquid medium have been studied and compared with geopolymers that use additional activating solutions as sodium or potassium hydroxide solutions (8 M), or a mixture of alkaline hydroxide and alkaline silicate solution ($NaOH–Na_2SiO_3$ or $KOH–K_2SiO_3$). The results showed that OPFA can be used as an alkaline activator, showing mechanical properties slightly lower than those obtained when additional alkaline hydroxide activating solutions were used. The best compressive strength was obtained for geopolymers that use alkaline silicates as an activating solution. However, the best thermal insulation properties were obtained for control geopolymers. The microstructural characteristics of the geopolymers were evaluated by means of X-ray diffraction (XRD), Fourier transform infrared (FTIR) spectroscopy and Scanning Electron Microscopy (SEM-EDS) that corroborate the formation of geopolymeric gel in all the specimens, being the amount of gel formed greater in samples using commercial potassium activating solutions. These results demonstrate the feasibility of using this type of waste, OPFA, as activating reagents in the manufacture of geopolymers or alkaline activated materials. The manufactured geopolymers can be used as compressed earth blocks for walls and partitions, since the specimens pursue mechanical properties that comply with current regulations, presenting better thermal insulation properties.

* Corresponding author.
E-mail address: deliche@ujaen.es (D. Eliche-Quesada).

https://doi.org/10.1016/j.jmrt.2021.03.102

1. Introduction

Geopolymers are low carbon binders obtained from the alkaline activation of natural minerals (clays), waste or industrial by-products to generate a product with ceramic characteristics [1,2]. The aluminosilicate type reactive materials dissolve rapidly in an alkaline solution and form hydroxylated oligomers of the type Si $(OH)_4$- and Al $(OH)_4^-$ [3,4]. During the polycondensation reaction, the tetrahedral units alternately join2 to form amorphous lattices that make up the geopolymers. In recent years, geopolymers have gained much attention as binders with lower energy consumption and powerful characteristics including good mechanical properties, low liquid permeability, resistance to high temperatures and acid attack among others [5] with a considerable reduction of CO_2 emissions, being more environmentally friendly materials [6–9].

Kaolin and other natural clays, after transformation by heat treatment into metakaolin and calcined clays, and low calcium fly ash are the most common precursors used in the synthesis of the geopolymers [10]. In recent years the focus has been on highly available raw materials, such as calcined clays [11,12]. Clay generally consists of a mixture of clay minerals and other associated ones [13]. Unlike kaolin, the main drawback of the clays use as a precursor for obtaining geopolymers is the variability in the composition and the control of the parameters that govern the thermal activation process. Common clays to be used as geopolymeric precursors, they must be calcined to complete dehydroxylation to avoid the formation of new stable phases, such as spinel [13–15]. Thermal activation of clay minerals between 500 and 800 °C generally results in dehydroxylation of the clay mineral [16]. Other authors have studied the alkaline activation of clays. Thus, Buchwald et al. [17] studied the suitability of illite/smectite clay thermally activated between 550 and 950 °C to form geopolymers. Essaidi et al. [18], studied the alkaline activation of a kaolinitic clay and a hematite-rich illite-kaolinitc clay activated at different temperatures. It is concluded that the reactivity of the illite-kaolinitc clay is superior to that of the kaolinitic clay due to the amorphization of the clay minerals, obtaining materials with better mechanical properties. Selmani et al. [9] evaluated two commercial metakaolins and three Tunisian clays, with different chemical composition, purity and reactivity, to determine their potential for geopolymer synthesis. The substitution of metakaolin by the clay favoured the polycondensation reaction.

The alkaline activators used are strongly alkaline solutions, alkali hydroxides or hydrated alkali silicates. However, the production of the alkaline silicates used as activators is carried out through very expensive and highly polluting economic processes, since temperatures above 1300 °C are required, emitting large amounts of CO_2 into the atmosphere. Therefore, the search for new alternative activating solutions is necessary, with less environmental and economic impact. One way to improve the economic and ecological balance of alkaline or alkaline activated cements would be to find substitutes (total or partial) for traditional alkaline activators.

In recent years, the use of biomass to generate heat and electricity, in order to apply waste and reduce CO_2 emissions to the atmosphere, has increased substantially in the European Union, becoming the fastest growing renewable energy. In Spain, biomass represents 5.21% of the total energy consumed [19]. The Andalusian Autonomous Community contains an important richness of biomass, coming from the olive crops and its derived industries. There are 1.52 million hectares of olive groves, which in an average campaign produce about 5.4 million tons of olives. This production is mainly devoted to the production of olive oil (92%), while the rest (approximately 8%) goes to table olives [20]. Two types of by-products or residues are generated in the two-phase production system for obtaining oil: wastewater and olive-pomace or "alpeorujo". The wastewater is derived from the vertical washing and centrifugal processes, as well as, to a lesser extent, from the cleaning of tanks, hoppers and other elements. The wastewater presents a large amount of waste, such as dust or dirt, oils and fats, sugars, nitrogenous substances, organic acids, polyalcohols and polyphenols. It is a highly contaminating material due to its acidity and high chemical oxygen demand (DQO) and biochemistry oxygen demand (DBO) [21]. The alpeorujo, or solid waste, is a paste formed by a mixture of pulp, bark, olive stone and residual oil. This residue has a high concentration of organic matter, oil and fat, and is rich in calcium and potassium [22]. The olive pomace industry has adapted to the reception of this by-product, from which an oil known as "olive-pomace oil" is obtained from a new centrifugation or by chemical extraction with solvent. After obtaining this oil, the remainder of the defatted alpeorujo or olive pomace can be used as an energy resource, such as biofuel, animal feed and agricultural fertilizers [23]. The combustion process used for the energy recovery of olive pomace generates large amounts of fly and bottom ash, whose final majority destination is abandonment in landfills, which leads to a waste problems and a strong environmental impact. Studies have been carried out on the potential use of olive pomace ash as raw material in the manufacture of cements, concretes, geopolymers and ceramic products [24–30].It is essential for a sustainable management to develop and optimize alternatives and low-cost technologies, which allow the reuse and recovery of ash. The olive pomace combustion ash is characterized by presenting a large amount of K_2O and CaO, having a high alkalinity in water suspension.

Most investigations using common clays as sources of aluminosilicates in the manufacture of geopolymers have studied the effect of heat treatment, the clays being activated using commercial activators. Therefore, the novelty of this investigation, is to study the use in the synthesis of alkaline activated materials or geopolymers olive pomace fly ash (OPFA) as potential source of alkalis to activate common clays. The binary system composed of a calcined clay (CC) from the Bailén quarries (Jaén, Spain) as a source of aluminosilicate and OPFA as an alkaline reagent using different activating solutions (water, NaOH (8 M), KOH (8 M) NaOH (8 M) -Na_2SiO_3 and KOH (8 M) -K_2SiO_3) has been analyzed. Therefore, it is intended to obtain new materials at low energy and with environmental advantages and the recovery of residues, such as fly ash from the olive pomace combustion as a sustainable alternative alkaline activator.

2. Materials and methods

2.1. Raw materials specifications

Clay belonging to the neogenic materials of the Guadalquivir basin was used as a source of aluminosilicates [31]. The clay has been supplied by Arcillas Bailén Company (Jaén, Spain). This raw material is dark gray. To obtain a uniform particle size, it was conditioned by crushing and grinding in a ball mill to produce a powder with a particle size suitable to pass through a 150 μm sieve. To increase its reactivity, the clay was heat treated at 750 °C (4 h) obtaining calcined clay (CC). The temperature of 750 °C was selected for the thermal treatment of the raw clay according to the thermogravimetric-thermodifferential analysis [32] (Cotes-Palomino et al., Kem diatoms). In the temperature range 450–630 °C, dehydroxylation of the silicates present in the clay takes place, while decomposition of the carbonates takes place at 750 °C. Therefore, a temperature of 750 °C was selected according to previous results obtained [33,34]. As alkaline activator, due to its richness in potassium, OPFA was used. The residue was supplied by the biomass plant "La Loma S.A." located in Villanueva del Arzobispo (Jaén, Spain). These ashes have a particle size of less than 150 μm and they do not require any pretreatment.

2.2. Sample preparation

In order to study the suitability of OPFA to perform as alkaline source for geopolymers synthesis, the binary system 70 wt% of CC and 30 wt% of OPFA were activated with water (control samples) using liquid/solid ratio = 0.4. For the purposes of comparison to a conventional activator, pastes were also prepared using a KOH solution; NaOH solution; a mix of a solution of sodium silicate and NaOH solution and anhydrous potassium silicate and KOH solution (8 M). Activating solutions were first prepared. For the preparation of the NaOH and KOH 8 M activating solutions, the necessary amount of NaOH (85 g) or KOH (137 g) pellets of 98 and 85% purity, respectively, was disolved by stirring magnetically in 260 ml of water. For the preparation of the activating solutions NaOH–Na_2SiO_3 and KOH–K_2SiO_3, the NaOH 8 M and KOH 8 M solutions were previously prepared and allowed to cool to room temperature prior to silicate addition. The appropriate amount of the sodium silicate solution (259 g) (29.2% SiO_2; 8.9% Na_2O and 61.9% H_2O) or potassium silicate solution (106 g), were prepared from the anhydrous potassium silicate (71.42% SiO_2 and 28.57% K_2O) and were added to the NaOH or KOH solution, respectively (Table 1). Activating solutions were allowed to cool under ambient conditions. Once the quantity of raw materials to be used has been optimized, the amount of each raw material is weighed corresponding to 70 wt % of CC and 30 wt % of OPFA. The raw materials were mixed in dry state in a Proeti S.A. planetary mixer at slow speed for 2 min. After this time, the alkaline activator was added, mixing the mixture for 10 min at fast speed. After kneading stage, the geopolymeric precursor was poured into 4 × 4 × 4 cm cubic silicone molds. The molds were filled in two batches, giving 60 knocking in each one on the Proeti S.A. shaking table to eliminate bubbles and achieve better compaction of the geopolymeric materials. The precursors were cured at 60 °C and 98% relative humidity for 24 h. After the first 24 h all the specimens were unmold and stored under ambient conditions (21 ± 2 °C and 58 ± 2% of relative humidity) for 28 days. 70 CC-30OPBA geopolymers (G) were identified by the type of alkaline activating solution used (Water (W); KOH (K), KOH–K_2SiO_3 (K-KSil); NaOH (Na) and NaOH–Na_2SiO_3 (Na-NaSil) (Fig. 1).

The composition of the mixture, and Si/Al (Na + K)/Si molar ratios are shown in Table 1. In all mixtures, the liquid/solid ratios were keep constant at 0.4. The liquid phase is formed by the water necessary for the preparation of the activating solutions and including the water contained in the sodium silicate solution, while solid phase is formed by the precursors (CC and OPFA).

2.3. Raw materials and geopolymers characterization

Particle size distribution of raw materials, CC and OPFA, was measured using a laser diffractometer Malvern Mastersizer

Table 1 – Molar ratio and dosage of the mixtures.

Sample	Si/Al	Na/Si	K/Si	(Na + K)/Si	CC(g)	OPFA (g)	NaOH (g)	KOH (g)	Na_2SiO_3 solution (g)	K_2SiO_3 (g)	Water (g)
G-W	2.97	0.02	0.61	0.61	455	195	–	–	–	–	260
G-Na	2.97	0.52	0.61	1.13	455	195	85	–	–	–	260
G-K	2.97	0.02	1.13	1.15	455	195	–	137	–	–	260
G-Na-NaSil	3.90	0.55	0.46	1.01	455	195	85	–	259		99
G-K-KSil	3.87	0.22	0.87	1.08	455	195	–	137	–	106	260

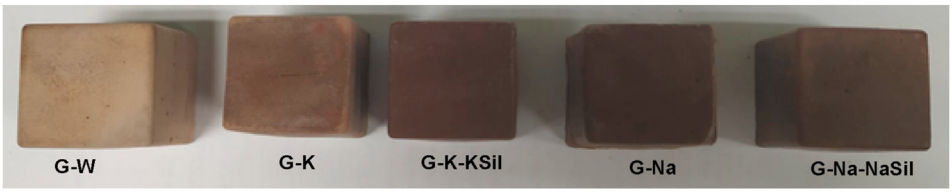

Fig. 1 – Photograph of 70C-30OPBA geopolymers using different activating solutions: Water (W); KOH (K), KOH–K_2SiO_3 (K-KSil); NaOH (Na) and NaOH–Na_2SiO_3 (Na-NaSil).

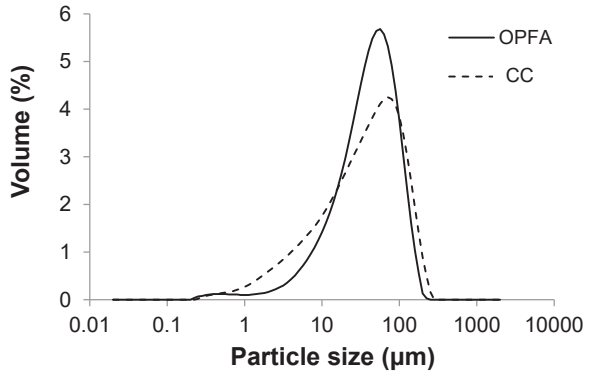

Fig. 2 – Particle size distribution of raw materials.

2000. The real density of the raw materials was determined with helium gas using an AccuPyc II 1340 pycnometer. The organic matter content of the precursors was determined according to ASTM D-2974 [35]. The carbonate content using a Bernard calcimetry. The determination of the chemical composition of the raw materials, was carried out using the X-ray fluorescence technique (XRF) using a Philips Magix Pro PW-2440 equipment. Crystalline mineralogical phases present in the raw materials and in the geopolymers after 28 days of curing were determined by the X-ray Diffraction technique (XRD) using an Empyrean X-ray powder diffraction equipment with a PIXcel-3D detector of PANalytical. HighScore software was used for the identification of crystalline phases. The degree of reaction of the geopolymers was determined by attack with HCl aqueous solution [36,37]. 1 g of geopolymer ground and sieved to a particle size of 150 mm was dissolved in an aqueous HCl solution (1:20). The solid was filtered, oven dried for 1 h and subsequently calcined at 1000 °C for 3 h. The aluminosilicate gel formed dissolves in the HCl solution, while the ash fraction remains in the insoluble residue. The degree of reaction provides an estimate of the amount of clay converted to geopolymer cement.

The bulk density determination was carried out according to the UNE-EN 772–13, 2001 standard [38]. The determination of the compressive strength was performed according to the UNE-EN 772-1 standard [39] using MTS 810 Material Testing Systems laboratory press. The determination of the thermal conductivity at of geopolymers at 20 °C was carried out with the heat flow meter FOX 50 TA Instruments in accordance with ISO 8302: 1991 [40]. Specimens with a thickness of 2 cm were used to evaluate the thermal conductivity, due to the equipment specifications. Fourier transform infrared spectroscopy (FTIR) spectra of raw materials and geopolymers have been performed with an FTIR Bruker Tensor 27 kit using the total attenuated reflection (ATR) method. Spectra were obtained between 4000 and 400 cm^{-1} using a resolution of 4 cm^{-1} in the absorbance mode. A JEOL SM 840 model scanning electron microscope (SEM) coupled with energy dispersive X-ray spectroscopy (EDS) device was used to examine the microstructures and chemical analysis of raw materials and geopolymers. The samples were placed on an aluminum rack and coated with carbon using the JEOL JFC 1100 sputtering coater.

3. Results and discussion

3.1. Characterization of raw materials

The particle size distribution of the OPFA, and the CC is shown in Fig. 2. The particle sizes of both raw materials are very similar, with an average particle size, D_{50}, 39.88 μm for C and 44.20 μm for OPFA. The percentage of fine particles (<2 μm) varies from 2.01 vol. % for OPFA to 3.92 vol. % for C. Both raw materials are made up of silt-sized particles (2–63 μm), 61.67 and 65.35 vol% for CC and OPFA, respectively. The content of sand particles (63–2000 μm) ranged between 34.42 vol % for C and 32.61 vol % for OPFA.

Table 2 shows the chemical composition of the raw materials determined by XRF analysis. It can be seen that the CC is mainly composed of SiO_2 (51.8%), Al_2O_3 (14.9%) and CaO (13.7%). The ratio between SiO_2 and Al_2O_3 contents is 3.48%. SiO_2 and Al_2O_3 are necessary compounds for the formation of geopolymers. So, clay can be used as a precursor. The OPFA is mainly composed of K_2O (52.1%), because potassium is the main component of olive pomace used as fuel. The residue contains hardly SiO_2 (~1.9%) and Al_2O_3 (~0.4%). This composition enable OPBA waste can be used as an alternative alkaline source for the activation of the clay. In addition the OPFA has a high value of loss on ignition (LOI), which indicates that it contains a high content of organic matter (5.1%), carbonates (31.2%) and hydrated phases, as well as the decomposition of inorganic compounds, with 6.8% SO_3.

The clay after heat treatment at 750 °C presents quartz, as the main crystalline mineralogical specie as identified by XRD, presenting in lower relative proportions X-ray peaks corresponding to calcite, feldspars and phyllosilicates such as illite and muscovite (Fig. 3a). The mineralogical characterization of OPFA (Fig. 3b) shows the presence of silvite (KCl), potassium sulfate or arcanite (K_2SO_4), dolomite ($CaMg(CO_3)_2$), calcium silicate o larnite (Ca_2SiO_4) and the carbonate kalicinite ($KH(CO_3)$).

3.2. Characterization of geopolymers

The bulk density of the 70C-30OPBA geopolymers after 28 curing days depending on the activating solution used is shown in Fig. 4. The bulk density values of the geopolymers are between 1343 and 1630 kg/m^3. The bulk density of the

Table 2 – Chemical composition of raw materials.

Raw materials	Chemical composition (wt %)											
	SiO_2	Al_2O_3	Fe_2O_3	CaO	MgO	K_2O	SO_3	MnO	Na_2O	TiO_2	P_2O_5	LOI
CC	51.80	14.9	4.95	13.70	2.01	2.89	5.53	0.02	0.80	0.84	0.13	2.20
OPFA	1.86	0.38	0.67	5.33	0.81	52.1	6.81	0.02	0.19	0.05	1.62	24.90

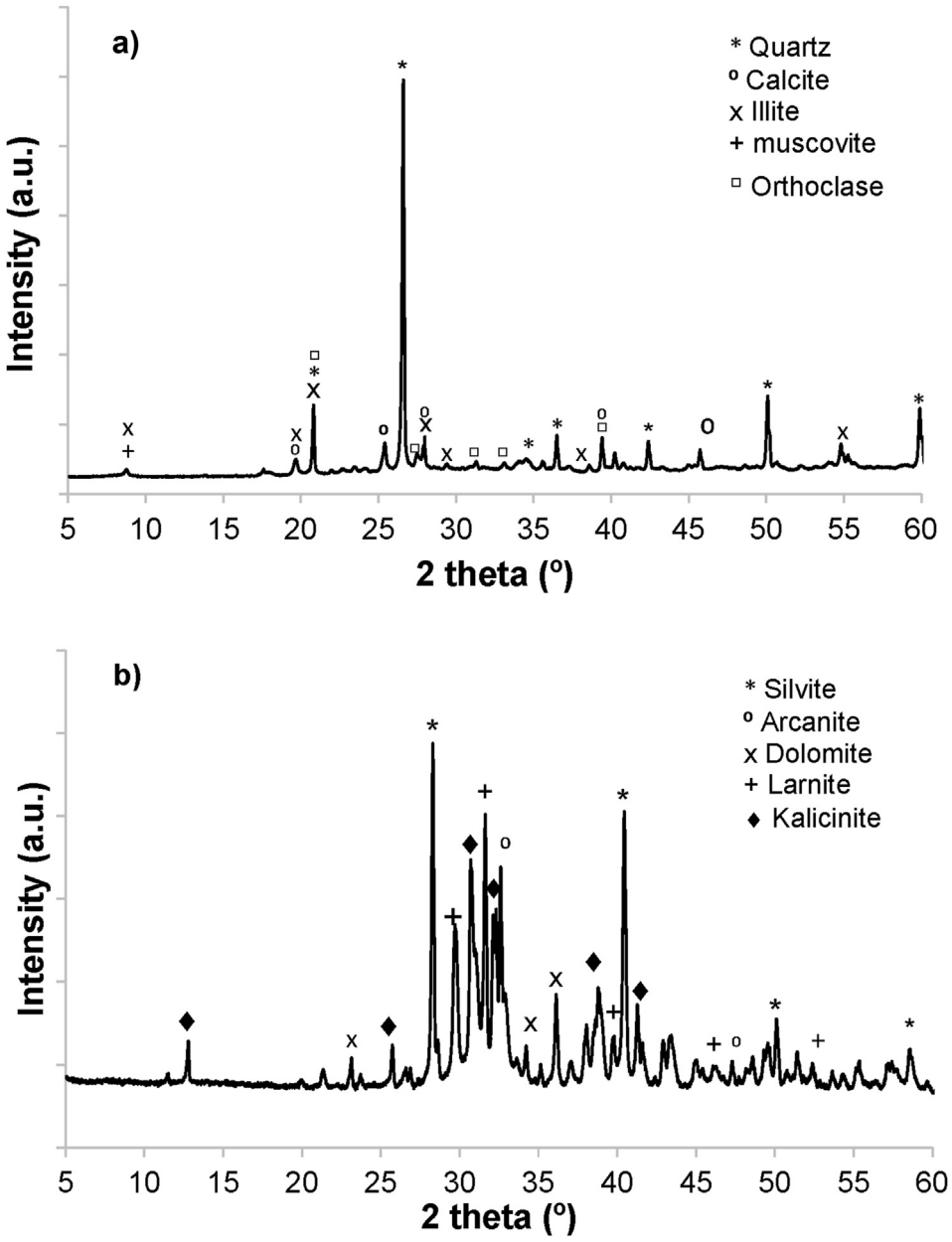

Fig. 3 – XRD patterns of raw materials (a) CC: calcined clay and (b) OPFA: olive pomace fly ash.

specimens is less than the real density of raw materials 2789 Kg/m^3 for clay and 2240 kg/m^3 for OPFA. Geopolymers with lower bulk density are those that use water, giving rise to a lighter structure. The use of activating solutions that incorporate sodium gives rise to geopolymers with a lower bulk density (1476–1584 kg/m^3) than the geopolymers obtained when the activating solution incorporates potassium (1509–1630 kg/m^3).

The addition of NaOH or KOH increases the bulk density of the activating solution with respect to using water. The addition of sodium or potassium silicate produces a further increase in the bulk density of the activating solution. Therefore, the increase in the bulk density of the geopolymers is in agreement with the increase in bulk density of the activating solutions. The denser geopolymers are those using

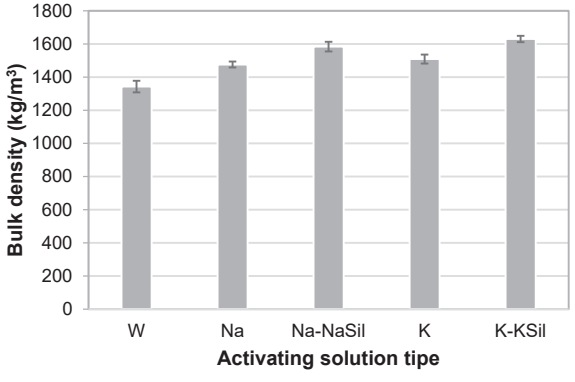

Fig. 4 – Bulk density of the 70C-30OPFA geopolymers cured 28 days as a function of alternative activating solution.

alkaline silicates (G-Na-NaSil and G-K-KSil). The increase in bulk density may also be due to the added soluble silicate, since the increase in silicon, as indicated by the Si/Al molar ratios, produces greater compaction and improvement of the physical properties [41]. In agreement with literature [42] alkaline silicate activation produces more compact geopolymers than those activated with hydroxide, possibly because silicates improve the condensation process of the ionic species produced in the geopolymer reaction system.

The compressive strength results of the geopolymers as a function of the type of activating solution used can be seen in Fig. 5. The G-W geopolymers have the lowest value of compressive strength (1.7 MPa). This could be due to the lower densification of these specimens and the lower formation of geopolymeric gel, as indicate the degree of reaction (56%) due to the low (Na + K)/Si molar ratio of 0.6. These low mechanical properties may be due to inadequate solubilization and low reactivity of the clay, which indicates insufficient amount of geopolymeric gel formed [43]. The systems with hydroxide, presenting greater values of compressive strength as compared to the control geopolymers. G-K geopolymers have greater compressive strength than G-Na geopolymers with a compressive strength of 3.9 and 3.0 MPa, respectively. The increase in compressive strength could be due to the increase in bulk density and to the largest amount of geopolymer gel formed according to the degree of reaction data (73.0 and 70.5%, respectively). K is more alkaline than Na, which can lead to greater dissolution of aluminosilicates [44] and the formation of a greater amount of geopolymeric gel. Therefore, K-activated systems are more efficient at the dissolution stage of the aluminosilicate than Na [44]. Furthermore, the addition of NaOH or KOH produced an increase of the (Na + K)/Si molar ratio that could influence the development of mechanical strength of geopolymers [43]. The ratio (Na + K)/Si is related to the degree of geopolymerization, since the alkali content must be sufficient to promote the solubilization of the aluminosilicates present in the clay raw material and alkalis present in the ash. A higher concentration of alkaline ions will lead to a higher dissolution rate of solid particles in the precursor, increasing the compressive strength [45,46]. The low mechanical performance of these geopolymers may be due both to the low reactivity of the clay and to its insufficient attack due to inadequate solubilization of the OPFA waste and the formation of an insufficient amount of aluminosilicate gel. Both G-Na and G-K specimens show a very slight increase of geopolymeric gel formation with respect to the G-W geopolymers that uses water, as indicated by the FTIR and XRD data. The geopolymers using silicate in addition to hydroxide as an activating solution have an increased compressive strength, which could be due to a higher degree of reaction and higher bulk density of the specimens. The use of the potassium silicate solution results in G-K-KSil geopolymers with the highest compressive strength values (9.0 MPa), being higher than for the geopolymers using sodium silicate (G-Na-NaSil) (5.3 MPa). The presence of soluble silica improves the mechanical properties. The increase in mechanical strength may be due to the fact that geopolymers based on potassium solutions have a lower porosity in their structure as indicate the bulk density data [47]. In the hydration of metal cations, it should be noted that the K^+ ions have a size of 1.33 Å, being slightly larger than the Na^+ ions with a size of 0.97 Å. This fact leads to a lower surface charge density in the case of K. Therefore, this difference in size will cause the K^+ to associate with more water molecules in the hydration process than the Na^+. This could indicate that larger cations may increase the degree of condensation during the formation of aluminosilicate structures [48]. Furthermore, the potassium solution is capable of dissolving more Al content compared to the sodium solution [49]. Xu and Deventer [50] studied the geopolymerisation of aluminosilicate minerals obtaining higher compressive strength after geopolymerisation in potassium than in sodium solutions. This fact could be due to a higher degree of condensation in the aluminosilicate structures prepared with potassium than those containing mainly sodium [51]. The higher degree of geopolymerization in K-containing geopolymers is corroborated by the degree of reaction. Geopolymers using potassium silicate G-K-KSil have higher degrees of reaction of 80.5% than geopolymers using sodium silicate Na (G-Na-NaSil) of 76.0%. The two activating solutions (K or Na) have similar pH values, but the alkali concentration is different. For the K-KSil activating solution the molar SiO_2/K_2O ratio is 0.7, while the molar SiO_2/Na_2O ratio is 0.9 for the Na-NaKSil activating solution. The dissolution in the geopolymerisation reaction increases for solutions with low silicon concentrations by improving the mass transport speed, so the percentage of unreacted material is low [52]. Therefore, the lower Si/K ratio could explain the higher amount of geopolymer gel shown by the potassium silicate systems. The compressive strength data indicate that the geopolymers have adequate values to be used as compressed earth block for walls and partitions [53]. According to their minimal mechanical compressive strength, the blocks are classified as BTC 1, BTC 3 and BTC 5 with minimum compressive strengths of 1.3, 3 and 5 MPa, respectively. Therefore, G-W geopolymers can be classified as BTC 1; G-Na and G-K as BTC 3 and G-Na-NaSil and G-K-KSil as BTC 5.

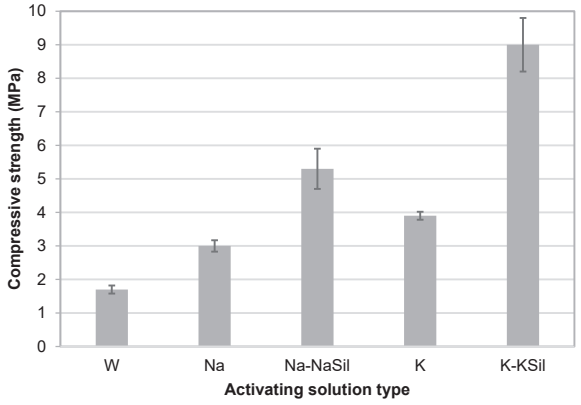

Fig. 5 – Compressive strength of the 70C-30OPFA geopolymers cured 28 days as a function of alternative activating solution.

The energy efficiency required in the field of construction has led to the development of insulating materials to improve the behaviour of new construction systems. The geopolymers that have the lowest thermal conductivity value, 0.317 W/mK, are control geopolymers that use only water, G-W

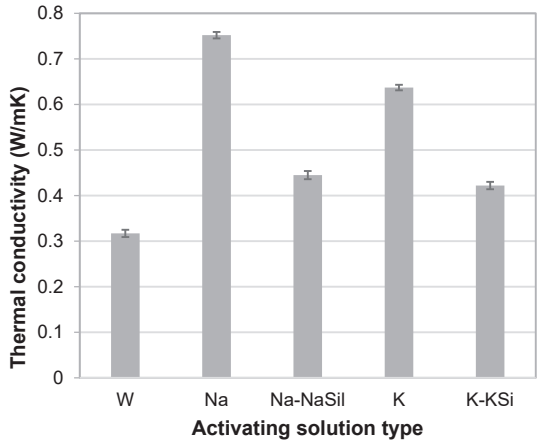

Fig. 6 – Thermal conductivity of the 70C-30OPFA geopolymers cured 28 days as a function of alternative activating solution.

geopolymers (Fig. 6), according to the bulk density data. Although for these geopolymers there is a relationship between bulk density and thermal conductivity, the same is not the case for specimens that use alkaline hydroxide or alkaline hydroxide and alkaline silicate as activating solution. The highest value of thermal conductivity is presented by geopolymers that use activating solutions of KOH and NaOH, with values of 0.637 and 0.752 W/mK for G-K and G-Na geopolymers, respectively (Fig. 6). The thermal conductivity of the geopolymers that use hydroxide and silicate as activating solutions are 0.422 and 0.445 W/mK for the G-K-KSil and G-Na-NaSil geopolymers, respectively. These data indicate that in addition to the bulk density of the geopolymers, other factors such as the nature of the gel formed, as well as the unreacted raw materials influence the thermal conductivity.

However, the geopolymers have a lower thermal conductivity and therefore a higher insulating capacity to compressed earth blocks with thermal conductivities of 1.1 W/mK [54].

Fig. 7 shows the XRD patterns of the geopolymers manufactured using different activating solutions for a curing time of 28 days. The diffraction peaks present in the raw materials (Fig. 3) can be observed. Diffraction peaks of quartz and calcite, mainly from clay and dolomite and larnite present in the OPFA, are present. In all the geopolymers, the diffraction peaks have less intensity that in the raw materials. The clay particles have been partially dissolved and the geopolymers obtained have a certain degree of crystallinity. They could still be detected by XRD after geopolymerization. It is also observed that no new crystalline phases appear in the geopolymerization process. A deviation in the baseline between 25° and 35° 2θ can be observed in all specimens, which indicates that during the geopolymerization reaction the geopolymeric gel constituted by amorphous aluminosilicates have been formed [55]. The gel phase is formed by dissolution from the surfaces of the alumino-silicate. The intensity of this halo increases in the following order G-W < G-Na < G-K < G-Na-NaSil < G-K-KSil (Fig. 7b–f). Increasing the intensity of the halo indicates increased geopolymeric gel formation which would lead to an increase in compressive strength. Geopolymers using potassium hydroxide and especially potassium silicate as activating solution, show a greater deviation from the baseline, indicating a greater proportion of amorphous material present in these specimens. Geopolymers using sodium as the alkaline medium have less geopolymer gel formation than the same geopolymers that use potassium. Na^+ ions are smaller in size than K^+, as above indicated, so Na^+ tend to form pair with smaller silicate oligomers, such as monomers. Such pairs, in turn, do not easily bind with another silicate anion. Thus, further formation of large silicate oligomers are not easy [56]. The larger size of the K^+ ion favours the formation of larger silicate in oligomers which Al $(OH)^-_4$ prefers to bind. Therefore, in solutions using potassium there are more geopolymer precursors that give rise to a better setting and a higher compressive strength of geopolymers than in the case of solutions using sodium [50].

The use of the alkaline silicate solution, mainly potassium, results in geopolymers with a greater amount of geopolymeric gel. The addition of alkaline silicate results in stronger formation of ion pairs, leading to a higher proportion of geopolymer precursors, more long chain silicate oligomers, as well as Al–O–Si complexes [57].

Fig. 8 shows the FTIR spectra of all geopolymers, as a comparison. The FTIR spectra of raw materials, CC and OPFA have been incorporated. The main bands observed in the FTIR spectra, associated with the bending and stretching modes of the main T-O bonds (where T is Si or Al) of the aluminosilicate structures, are indicated in Table 3. The bands centred between 950 and 1050 cm^{-1} are attributed to the asymmetric stretching of the T-O bonds (T = Si or Al) [58–60]. These vibrations take place in the Si and Al tetrahedral which are the main building blocks of the aluminosilicate structures, and therefore, represent the fingerprint of the geopolymerization reaction process. The displacement of the T-O bands in the geopolymers at higher energies (988-993 cm^{-1}) shows that the silicates in the precursor clay (983 cm^{-1}) have participated in the geopolymerisation reaction by forming aluminosilicate geopolymer gels. The values obtained are quite similar, although there seems to be a slight shift to higher energies in the case of the matrix containing only K. G-K geopolymers have a higher wavenumbers of T-O link stretching than G-Na geopolymers. The trend is the same when comparing specimens that also use G-Na-NaSil and G-K-KSil. For samples using alkaline potassium solutions, higher band wavenumbers may indicate a higher degree of polycondensation due to the presence of K. These data support the results of the compressive strength, as well as the higher degree of condensation of the K^+ due to its size and coordination with the water molecules.

In the FTIR spectra of geopolymers using traditional activating solutions, another absorption band is observed centred between 1103 and 1123 cm^{-1}. They are assigned to the asymmetric stretching of bonds between tetrahedral Si–O–Si, which in turn depends on the Si/Al ratio [61], therefore, it would be influenced by changes in the structural framework. In the geopolymers containing K, higher wavenumbers are again observed than the matrices containing mainly sodium. Geopolymers with sufficient K serve to strengthen the bonds

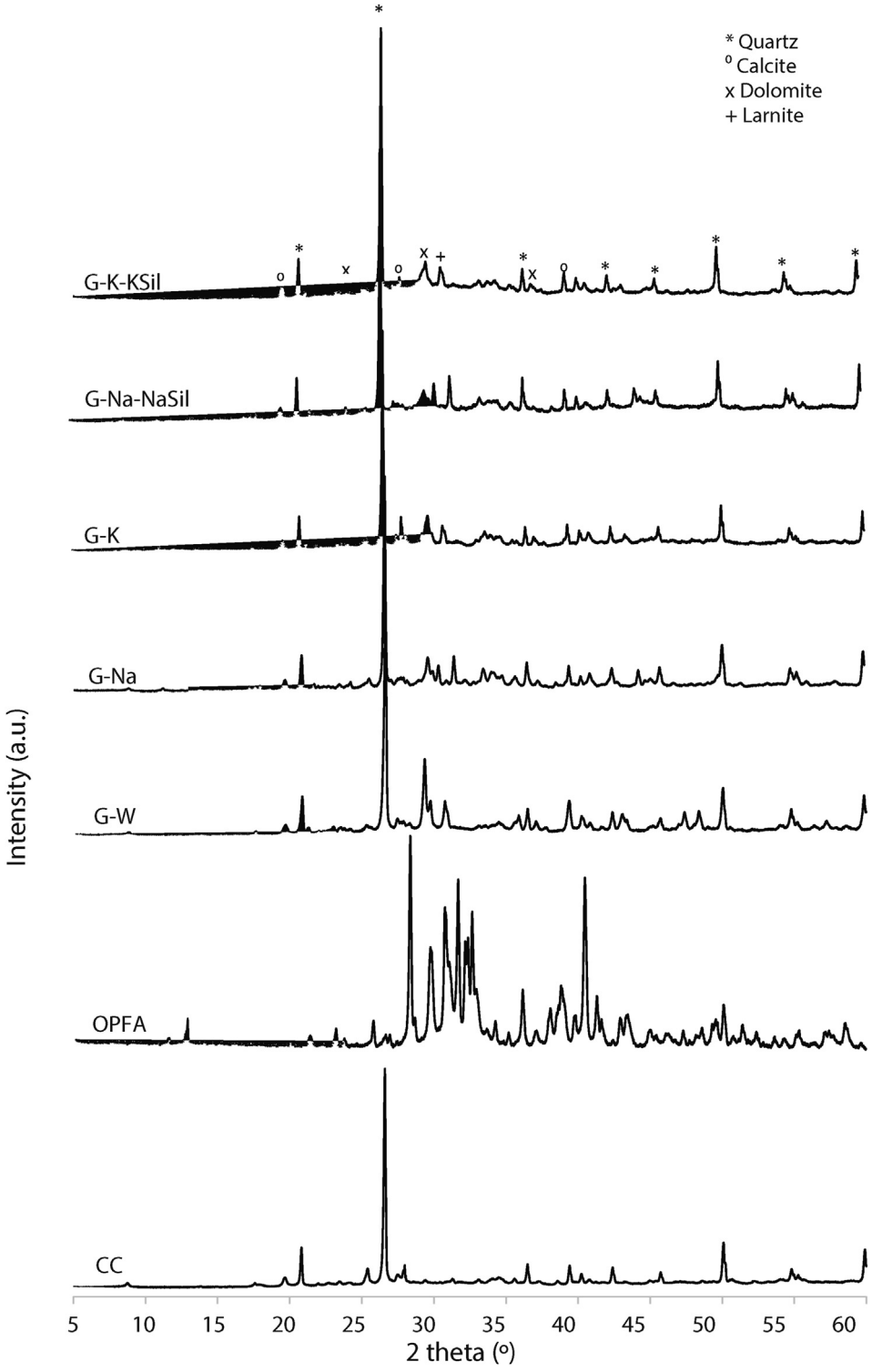

Fig. 7 – XRD patters of 70C-30OPFA geopolymers with various additional activating solutions.

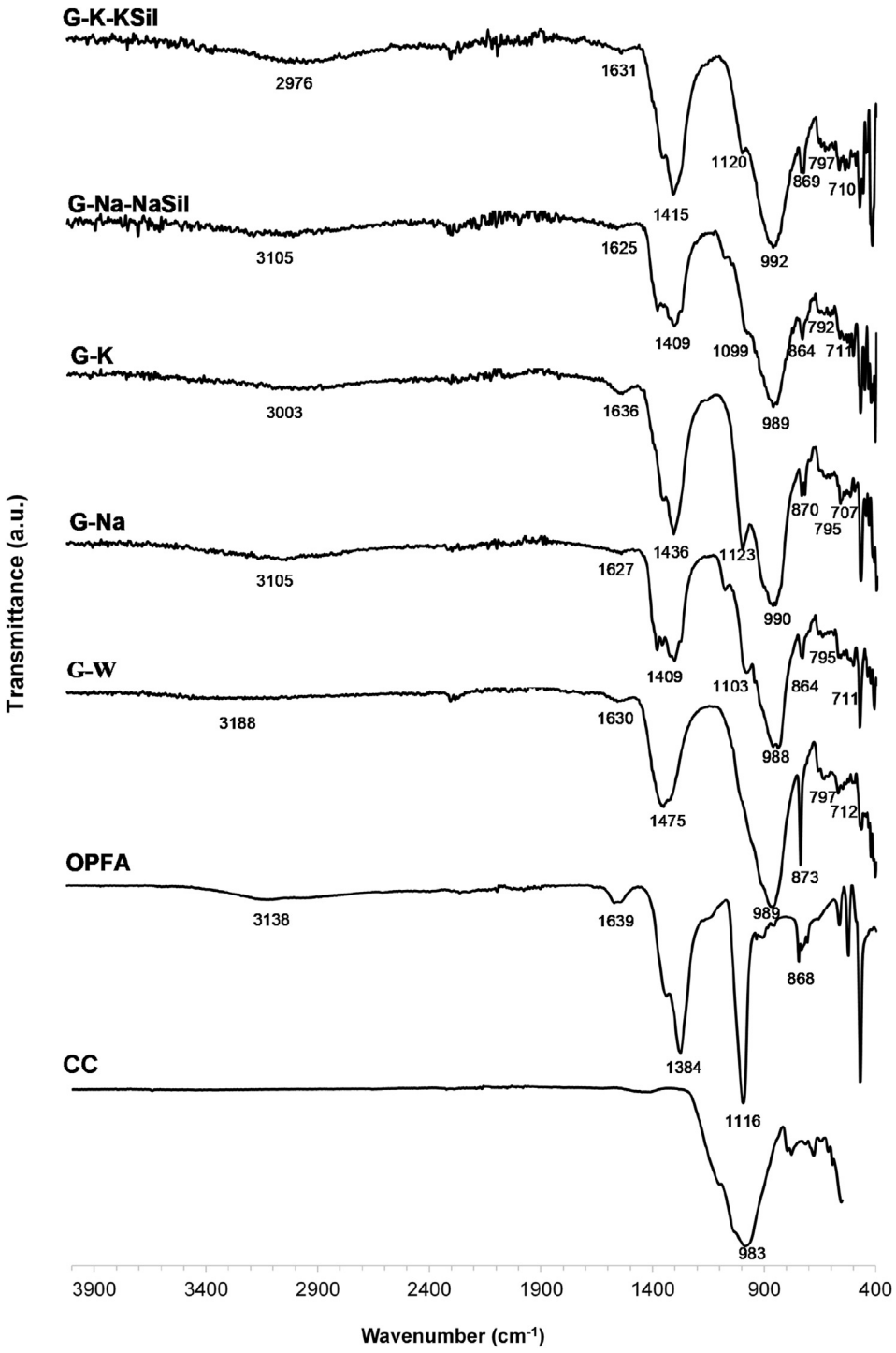

Fig. 8 – IR spectra of 70C-30OPFA geopolymer products with various additional activating solutions.

Table 3 – FTIR results of raw materials and geopolymer for selected bands (cm^{-1}).

Geopolymers	Si–O–Al(Si) (asymmetric stretching vibrations	Si–O–Si (asymmetric stretching vibrations)	Si–O–Si (symmetric stretching vibrations)	Si–O–Al(Si) (symmetric stretching vibrations)
CC	983	–	–	–
OPFA	–	1116	–	–
G-W	989	–	797	712
G-Na	988	1103	795	711
G-K	990	1123	795	707
G-Na-NaSil	989	1099	792	711
G-K-KSil	992	1120	797	710

between these secondary construction units, a fact that is represented in the compressive strength results [51].

In all geopolymers, wide absorption bands can be seen centred at approximately 2976–3188 cm^{-1}. They correspond to the chemical bonding stress –OH vibration of the free water molecules or physically absorbed at the surface or into the pores of the gel. The second band centred between 1636 and 1625 cm^{-1} is attributed to the bending vibration of the vibratory transition of the H–O – H bonds [62,63]. Apparently, these bands show the absorption of closed water in the sample cavities or water from the surface of the geopolymer structure [64]. These bands show a small difference in intensity depending on the alkaline activator used, being slightly more intense in geopolymers using potassium as the activating solution compared to those using the same activating solution but sodium. It can probably be due to a greater dissolution of the clay, resulting in the formation of more hydrated compounds [65].

The absorption bands in the range 1475–1409 cm^{-1}, as well as, the bands in the range 873–864 cm^{-1} are related to the

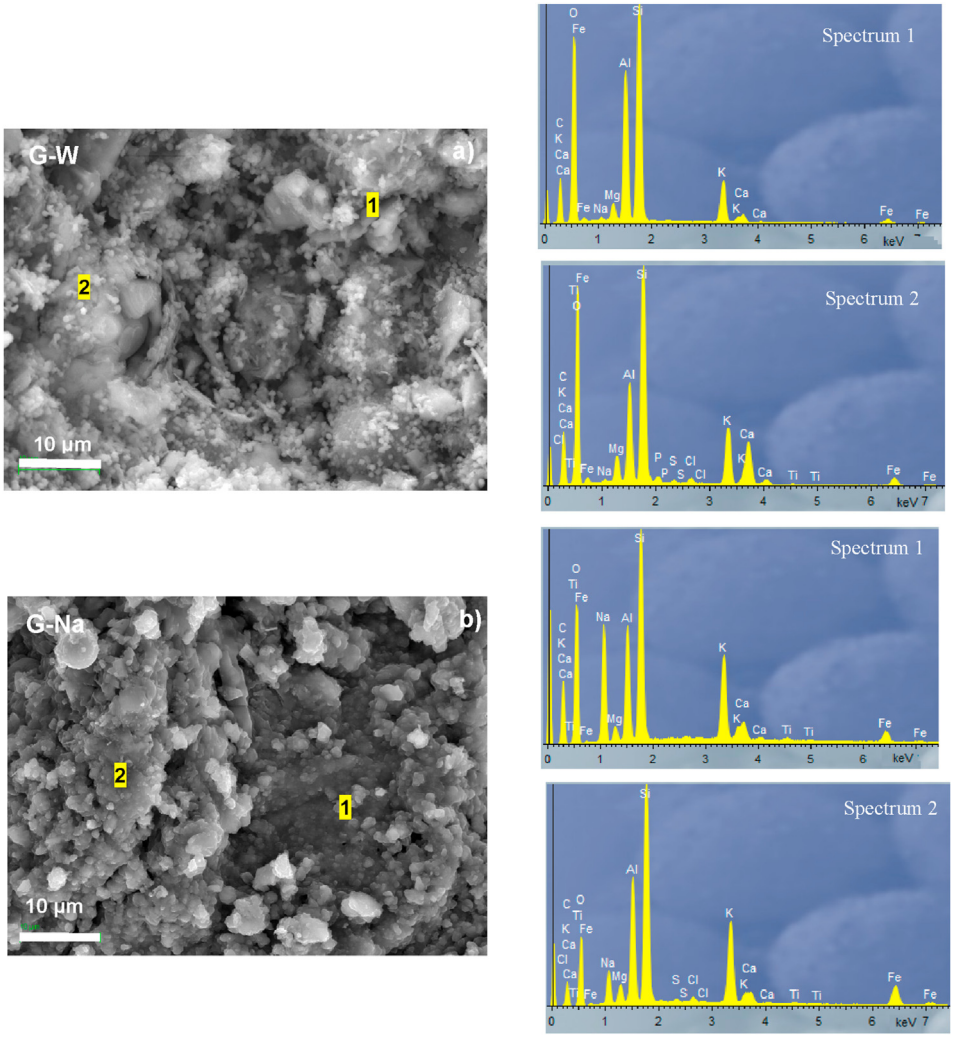

Fig. 9 – Selected SEM images andEDS analysis of (a) G-W geopolymers; (b) G-Na geopolymers; (c) G-K geopolymers; (d) G-Na-NaSil geopolymers and G-K-KSil geopolymers at 5000X.

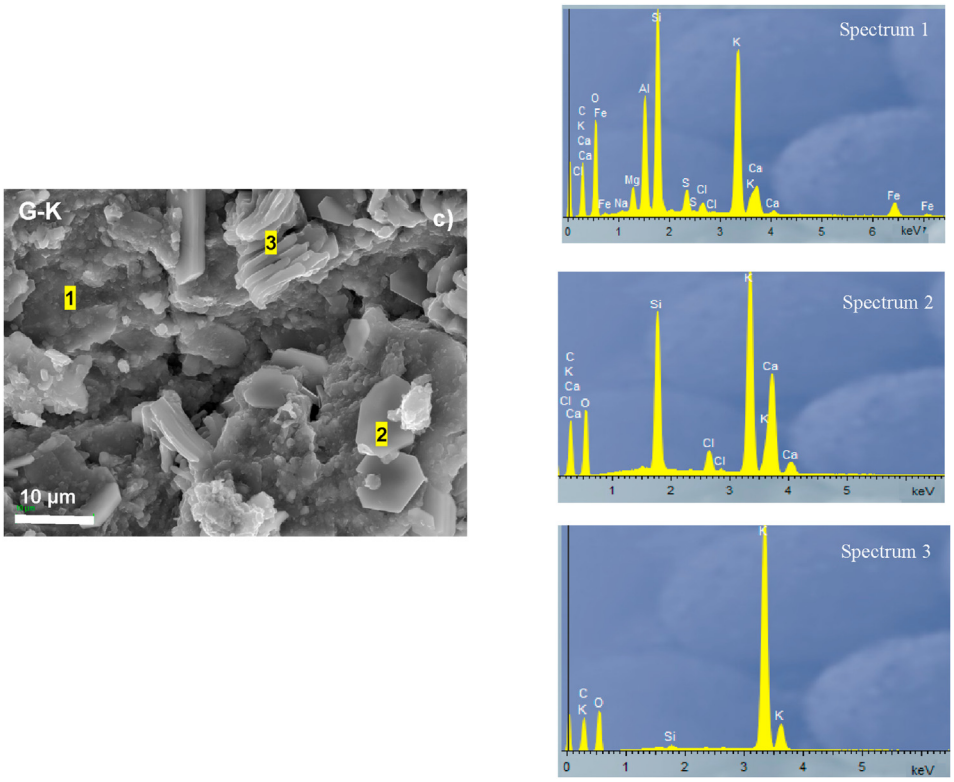

Fig. 9 – (*continued*).

vibrations of CO_3^{2-} carbonate. The former are due to the asymmetric stretching vibrations of O–C–O bond, and the latter to out-of-plane bending vibrations [66], which indicates atmospheric carbonation, which can lead to the appearance of efflorescence in the samples. Excess sodium and potassium in the matrix can react with atmospheric CO_2 to give rise to carbonates or sodium or potassium bicarbonates [67]. In the region between 800 and 700 cm^{-1} it can be observed centred bands due to the symmetric stretching vibrations of Si–O–Si and Si–O–Al(Si) bonds which again indicate the presence of amorphous silicates [68].

In general, it can be distinguished FTIR bands due to vibrations related to the OH- groups of water centred in the range 3200–3000 cm^{-1} and in the range 1636–1625 cm^{-1}, bands assigned to carbonate vibrations in the range 1409–1480 cm^{-1}, as well as in the range 873–864 cm^{-1}, and bands related to Si–O(Al) group vibrations in the range 1100–450 cm^{-1}.

C-OPFA geopolymers can be described as systems consisting of binder geopolymeric gel surrounded by non-reactive particles of the raw materials, mainly clay, indicating a partial dissolution of the clay by the OPFAs and by the additional activating solutions for form the geopolymer. In addition, in all of them, open and closed pores were observed by SEM (Fig. 9). It can be seen that in the control geopolymers (Fig. 9a) and in the geopolymers that use NaOH (Fig. 9b) the development of geopolymeric gel is more limited. In general, no significant differences are observed in the appearance of the control geopolymer (G-W) and the geopolymer that uses NaOH (G-Na) that have low reactivity and limited activation. They present a porous microstructure that consists of a geopolymeric gel surrounded by particles of unreacted raw materials. The use of KOH (G-K geopolymers) changes the microstructure, observing a homogeneous amorphous geopolymeric gel matrix surrounded by unreacted particles (Fig. 9c). The addition of silicate changes the microstructure to a greater extent, observing a denser structure due to the greater amount of amorphous phase or hydrated aluminosilicate gel (N-A-S-H or K-A-S-H gel) (Fig. 9 d and e). A greater degree of development of geopolymers is observed, due to dissolution of the clay not only by the OPFA, but also by the alkaline activator. In general, no significant differences in appearance were observed in G-Na-NaSil and G-K-KSil geopolymers regardless of whether sodium or potassium silicate is used. However, a greater amount of unreacted particles can be observed in G-Na-NaSil geopolymers. Furthermore, due to the higher Si/Al ratio of these geopolymers, shrinkage microcracks were visible.

The elemental chemical composition of the aluminosilicate gel is mainly based on a majority content of silicon, aluminium and potassium and/or sodium and small percentages of calcium and magnesium. EDS analysis indicates that the gel composition varies depending on the activator used.In all samples using a potassium source as an alkaline activator of calcium aluminosilicate hydrates rich in potassium K(C)A-S-H gel areas. In G-K geopolymers, hexagonal structures rich in K, Si, Ca and Cl were also observed, as well as other rich in K. In geopolymers that use sodium-rich

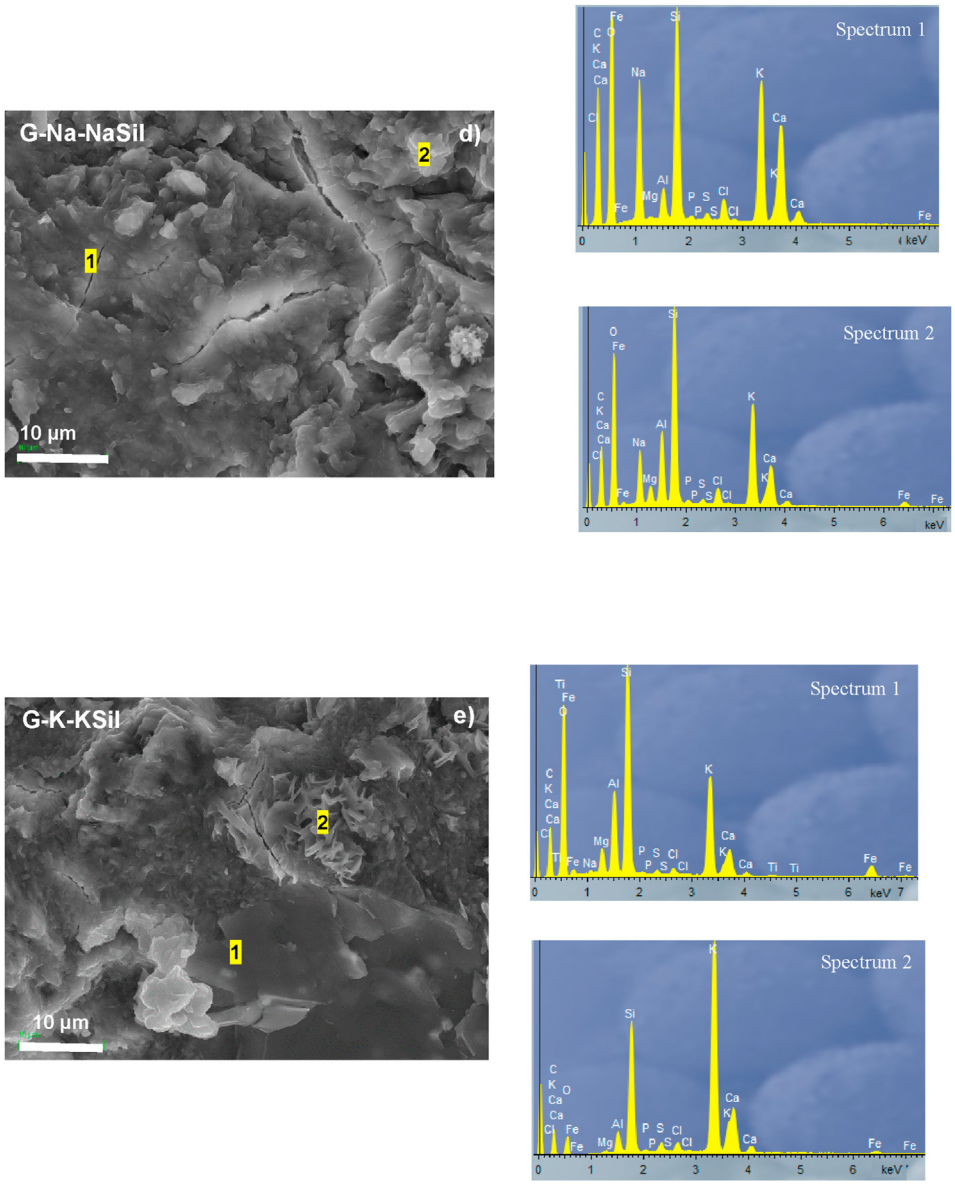

Fig. 9 – *(continued)*.

sources as a commercial alkaline activator, the gel is also enriched in this alkaline metal, being observed the formation of K–N(C)A-S-H gel areas.

4. Conclusions

. From the results obtained, the following conclusions can be drawn:

- The bulk density of the geopolymers increases as the density of the activating solution used increases, improving the presence of alkaline silicates the condensation process of the ionic species.
- The compressive strength of control geopolymers is 1.3 MPa. The use of alkaline hydroxides results in an increase in the compressive strength, increasing it to 3.0–3.9 MPa. Control geopolymers and those using NaOH have a microstructure with a lower amount of geopolymer gel. The highest values of compressive strength (5.3–9.0 MPa) are obtained when an alkaline hydroxide/alkaline silicate activating solution is used. The geopolymers using KOH, and mainly those used in addition to alkaline hydroxide silicate, have a greater amount of geopolymer gel. The geopolymers using potassium as an activating solution obtain better values of compressive strength. It is found that the type of alkaline cation affects the geopolymerisation of the clay. The larger size of the K^+ results in a higher degree of condensation compared to Na^+ under the same conditions, as indicated by the XRD and FTIR results. Geopolymers comply with the regulations to be used as compressed earth blocks for walls and partitions.

The geopolymers obtained have thermal conductivity values between 0.317 and 0.752 W/mK. The geopolymers with the highest insulation capacity are the control geopolymers using H_2O (G-W specimens).

Therefore, these data indicate that OPFA can be used as an alkaline source to activate CC, obtaining geopolymers with suitable physical and thermal properties but with low mechanical properties. The use of activating solutions that use commercial alkaline silicates leads to a greater dissolution of the clay, resulting in the formation of a greater proportion of geopolymeric gel, giving alkali activated materials with better mechanical properties. In this system the type of alkali to be used in the synthesis will depend on the final objective in terms of application, obtaining better mechanical properties when potassium activating solutions are used.

Declaration of Competing Interest

The authors declare that they have no known competing financial interests or personal relationships that could have appeared to influence the work reported in this paper.

Acknowledgements

This work has been funded by the project *Development and characterization of new geopolymeric composites based on waste from the olive industry. Towards a sustainable construction* (MAT2017-88097-R), FEDER/Ministry of Science, Innovation and Universities, State Research Agency. The authors thank "Arcillas Bailen" company and Energía La Loma S.A. for supplying the clay and olive pomace fly ash, respectively. M.A. Gómez-Casero acknowledges support of MINECO (PRE2018-084073). Technical and human support provided by CICT of Universidad de Jaén (UJA, MINECO, Junta de Andalucía, FEDER) is gratefully acknowledged.

REFERENCES

[1] Catauro M, Tranquillo E, Barrino F, Dal Poggetto G, Blanco I, Cicala G, et al. Mechanical and thermal properties of fly ash-filled geopolymers. J Therm Anal Calorim 2019;138:3267–76. https://doi.org/10.1007/s10973-019-08612-y.

[2] Lee W-H, Lin K-L, Chang T-H, Ding Y-C, Cheng T-W. Sustainable development and performance evaluation of marble-waste-based geopolymer concrete. Polymers 1924;2020:12. https://doi.org/10.3390/polym12091924].

[3] Grutzeck MW, Siemer DD. Zeolites synthesised from class F fly ash and sodium aluminate slurry. J Am Ceram Soc 1997;80(9):2449–58. https://doi.org/10.1111/j.1151-2916.1997.tb03143.x.

[4] Davidovits J. Geopolymer. Chemistry and applications. 3th ed. Saint-Quentin, Francia: Institut Geopolymer; 2008.

[5] Duxson P, Fernández-Jiménez A, Provis JL, Lukey GC, Palomo A, van Deventer JSJ. Geopolymer technology: the current state of the art. J Mater Sci 2007;42(9):2917–33. https://doi.org/10.1007/s10853-006-0637-z.

[6] Nath SK. Fly ash and zinc slag blended geopolymer: immobilization of hazardous materials and development of paving blocks. J Hazard Mater 2020;387:121673. https://doi.org/10.1016/j.jhazmat.2019.121673.

[7] Ye N, Chen Y, Yang J, Liang S, Hu Y, Xiao B, et al. Co-disposal of MSWI fly ash and Bayer red mud using an one-part geopolymeric system. J Hazard Mater 2016;2016(318):70–8. https://doi.org/10.1016/j.jhazmat.2016.06.042.

[8] Autef A, Joussein E, Poulesquen A, Gasgnier G, Pronier S, Sobrados I, et al. Influence of metakaolin purities on potassium geopolymer formulation: the existence of several networks. J Colloid Interface Sci 2013;408:43–53. https://doi.org/10.1016/j.jcis.2013.07.024.

[9] Selmani S, Essaidi N, Gouny F, Bouaziz S, Joussein E, Driss A, et al. Physical-chemical characterization of Tunisian clays for the synthesis of geopolymers materials. J Afr Earth Sci 2015;103:113–20. https://doi.org/10.1016/j.jafrearsci.2014.12.009.

[10] Liew YM, Heah CY, Mohd-Mustafa AB, Kamarudin H. Structure and properties of clay-based geopolymer cements: a review. Prog Mater Sci 2016;83:595–629. https://doi.org/10.1016/j.pmatsci.2016.08.002.

[11] Seiffarth T, Hohmann M, Posern K, Ch Kaps. Effect of thermal pre-treatment conditions of common clays on the performance of clay-based geopolymeric binders. Appl Clay Sci 2013;73:35–41. https://doi.org/10.1016/j.clay.2012.09.010Get.

[12] El Hafid K, Hajjaji M. Effects of the experimental factors on the microstructure and the properties of cured alkali-activated heated clay. Appl Clay Sci 2015;116–117:202–10. https://doi.org/10.1016/j.clay.2015.03.015.

[13] Buchwald A, Hohmann M, Posern K, Brendler E. The suitability of thermally activated illite/smectite clay as raw material for geopolymer binder. Appl Clay Sci 2009;46:300–4. https://doi.org/10.1016/j.clay.2009.08.026.

[14] Bergaya F, Dion P, Alcover JF, Clinard C, Tchoubar D. TEM study of kaolinite thermal decomposition by controlled-rate thermal analysis. J Mater Sci 1996;31:5069–75. https://doi.org/10.1007/BF00355907.

[15] Hamdi N, Messaoud IB, Srasra E. Production of geopolymer binders using clay minerals and industrial wastes. Compt Rendus Chem 2019;22(2–3):220–6. https://doi.org/10.1016/j.crci.2018.11.010.

[16] Heller-Kallai L. Handbook of clay science, Development in Clay science. In: Bergaya F, Theng BKG, Lagaly G, editors. Thermally modified clay minerals. Amsterdam: Elsevier; 2006. p. 289–308.

[17] Buchwald A, Hohmann M, Posern K, Brendler E. The suitability of thermally activated illite/smectite clay as raw material for geopolymer binders. Appl Clay Sci 2009;46(3):300–4. https://doi.org/10.1016/J.CLAY.2009.08.026.

[18] Essaidi N, Samet B, Baklouti S, Rossignol S. Feasibility of producing geopolymers from two different Tunisian clays before and after calcination at various temperatures. Appl Clay Sci 2014;88–89:221–7. https://doi.org/10.1016/j.clay.2013.12.006.

[19] European Biomass Association. http://biomassmagazine.com/articles/13837/european-biomass-association-releases-2016-bioenergy-outlook. [Accessed 15 November 2020].

[20] Plan Director del olivar andaluz. Consejería de Agricultura, pesca y desarrollo rural. Junta de Andalucía. 2017. https://www.juntadeandalucia.es/export/drupaljda/Plan%20Director%20del%20Olivar.pdf. [Accessed 16 November 2020].

[21] Romero E, Quirantes M, Nogales R. Characterization of biomass ashes produced at different temperatures from olive-oil-industry and greenhouse vegetable wastes. Fuel 2017;208:1–9. https://doi.org/10.1016/j.fuel.2017.06.133.

[22] Vlyssides AG, Loizides M, Karlis PK, Clean J. Integrated strategic approach for reusing olive oil extraction by-products. J Clean Prod 2004;12:603–11. https://doi.org/10.1016/S0959-6526(03)00078-7.

[23] Roig A, Cayuela ML, Sánchez-Monedero MA. An overview on olive mil wastes and their valorisation methods. Waste

Manage 2006;26:960–9. https://doi.org/10.1016/j.wasman.2005.07.024Get.
[24] Cuenca J, Rodríguez J, Martín-Morales M, Sánchez-Roldán Z, Zamorano M. Effects of olive residue biomass fly ash as filler in self-compacting concrete. Construct Build Mater 2013;40:702–9. https://doi.org/10.1016/j.conbuildmat.2012.09.101.
[25] Cruz-Yusta M, Mármol I, Morales J, Sánchez L. Use of olive biomass fly ash in the preparation of environmentally friendly mortars. Environ Sci Technol 2011;45:6991–6. https://doi.org/10.1021/es200968a.
[26] Fernández-Pereira C, de la Casa JA, Gómez-Barea A, Arroyo F, Leiva C, Luna Y. Application of biomass gasification fly ash for brick manufacturing. Fuel 2011;90:220–32. https://doi.org/10.1016/j.fuel.2010.07.057.
[27] Eliche-Quesada D, Leite-Costa J. Use of bottom ash from olive pomace combustion in the production of eco-friendly fired clay bricks. Waste Manag 2016;48:323–33. https://doi.org/10.1016/j.wasman.2015.11.042.
[28] Pérez-Villarejo P, Eliche-Quesada D, Carrasco-Hurtado B, Sánchez-Soto PJ. Valorization of olive biomass fly ash for production of eco friendly ceramic bricks. Encyclopedia of Renewable and Sustainable Materials 2020;5:285–94. https://doi.org/10.1016/B978-0-12-803581-8.11547-4.
[29] Font A, Soriano L, S Moraes Pinheiro M-dM, Tashima MM, Monzó J, Borrachero MV, et al. Design and properties of 100% waste-based ternary alkali-activated mortars: blast furnace slag, olive-stone biomass ash and rice husk ash. J Clean Prod 2020;118568:243. https://doi.org/10.1016/j.jclepro.2019.118568.
[30] Alonso MM, Gascó C, Martín Morales M, Suárez-Navarro JA, Zamorano M, Puertas F. Olive biomass ash as an alternative activator in geopolymer formation: a study of strength, radiology and leaching behavior. Cement Concr Compos 2019;103384:104. https://doi.org/10.1016/j.cemconcomp.2019.103384.
[31] Vázquez M, Jiménez-Millán JJ. Materias primas ricas en arcilla de las capas rojas triásicas (norte de Jaén, España) para fabricar materiales cerámicos de construcción. Mater Constr 2004;273:5–20.
[32] Cotes-Palomino MT, Martínez-García C, Eliche-Quesada D, Pérez-Villarejo L. Production of ceramic material using wastes from brewing industry. Key Eng Mater 2016;663:94–104. 10.4028/www.scientific.net/KEM.663.94.
[33] Eliche-Quesada D, Bonet-Martínez E. Pérez-villarejo L,castro E, sánchez-soto PJ. Effects of an illite clay substitution on geopolymer synthesis as an alternative to metakaolin. J Mater Civ Eng 2021;33(5):04021072.
[34] Heller-Kallai L. Thermally modified clay minerals. In: Bergaya F, Theng BKG, Lagaly G, editors. Handbook of clay science, Development in Clay science. Amsterdam: Elsevier; 2006. p. 289–308. https://doi.org/10.1061/(ASCE)MT.1943-5533.0003690.
[35] ASTM D2974–20e1,. Standard test methods for determining the water (moisture) content, ash content, and organic material of peat and other organic soils. West Conshohocken, PA: ASTM International; 2020.
[36] Fernández-Jiménez A, Palomo A, Criado M. Microstructure development of alkali activated Fly ash cement: a descriptive model. Cem Concr Res 2005;35:1204–9. https://doi.org/10.1016/j.cemconres.2004.08.021.
[37] Fernández-Jiménez A, de la Torre AG, Palomo A, López-Olmo G, Alonso MM, Aranda MAG. Quantitative determination of phases in the alkaline activation of fly ash. Part II: degree of reaction. Fuel 2006;85:1960–9. https://doi.org/10.1016/j.fuel.2006.04.006.
[38] UNE-EN 772–813. Methods of test for masonry units - Part 13: determination of net and gross dry density of masonry units (except for natural stone). 2001.
[39] UNE-EN 772–781. Methods of test for masonry units - Part 1: determination of compressive strength.. 2011.
[40] ISO 8302:. Thermal insulation — determination of steady-state thermal resistance and related properties — guarded hot plate apparatus. 1991.
[41] Kovalchuck G, Fernández-Jiménez A, Palomo A. Alkali activated fly ash. Relationship between mechanical strength gains and initial ash chemistry. Mater Constr 2006;58(291):35–52. https://doi.org/10.3989/mc.2008.v58.i291.101.
[42] Kovalchuck G, Fernández-Jiménez A, Palomo A. Alkali activated fly ash. Relationship between mechanical strength gains and initial ash chemistry. Mater Constr 2008;58:35–52. https://doi.org/10.3989/mc.2008.v58.
[43] Silva de Vargas DCC, Dal Molin A, Vilela CF, da Silva FJ, Pavão B, Veit H. The effects of Na_2O/SiO_2 molar ratio, curing temperature and age on compressive strength, morphology and microstructure of alkali-activated fly ash-based geopolymers. Cem Concr 2011;33:653–60. https://doi.org/10.1016/j.cemconcomp.2011.03.006t.
[44] Sindhunata Van Deventer JSJ, Lukey GC, Xu H. Effect of curing temperature and silicate concentration on fly ash-based geopolymerization. Ind Eng Chem Res 2006;45:3559–68. https://doi.org/10.1021/ie051251p.
[45] Leong HY, Ong DEL, Sanjayan JG, Nazari A. The effect of different Na_2O and K_2O ratios of alkali activator on compressive strength of fly ash based-geopolymer. Constr Build Mater 2016;50011:106. https://doi.org/10.1016/j.conbuildmat.2015.12.1-41.
[46] Luukkonen T, Abdollahnejad Z, Yliniemi J, Kinnunen P, Illikainen M. One-part alkali activated materials: a review. Cem Concr Res. 2018;103:21–34. https://doi.org/10.1016/j.cemconres.2017.10.001.
[47] Lizcano M, Kim HS, Basu S, Radovic M. Mechanical properties of sodium and potassium activated metakaolin-based geopolymers. J Mater Sci 2012;47:2607–16. https://doi.org/10.1007/s10853-011-6085-4.
[48] McCormick AV, Bell T. The solution chemistry of zeolite precursors. Catal Rev Sci Eng 1989;97:31. https://doi.org/10.1080/01614948909351349.
[49] van Jaarsveld JGS, van Deventer JSJ, Lukey GC. The characterisation of source materials in fly ash-based geopolymers. Mater Lett 2003;57:1272–80. https://doi.org/10.1016/S0167-577X(02)00971-0.
[50] Xu H, van Deventer JSJ. The geopolymerization of alumino-silicate minerals. Int J Miner Process 2000;59:247–66. https://doi.org/10.1016/S0301-7516(99)00074-5.
[51] van Jaarsveld JGS, van Deventer JSJ. Effect of the alkali metal activator on the properties of fly ash-based geopolymers. Ind Eng Chem Res 1999;38:3932–41. https://doi.org/10.1021/ie980804b.
[52] Duxson P, Lukey GC, Separovic F, van Deventer JSJ. Effect of alkali cations on aluminum incorporation in geopolymeric gels. Ind Eng Chem Res 2005;2005(44):832–9. https://doi.org/10.1021/ie0494216.
[53] UNE 41410. Compressed earth blocs for walls and partitions. Definitions, specifications and test methods. 2008.
[54] UNE-EN 1745. Masonry and masonry products - methods for determining thermal properties. 2013.
[55] Barbosa VF, Mackenzie KJD. Synthesis and characterization of materials inorganic polymers. Int J Inorg Mater 2000;2(4):309–17. https://doi.org/10.1016/S1466-6049(00)00041-6.
[56] Hendricks WM, Bell AT, Radke CJ. Effect of organic and alkali metal cations on the distribution of silicate anions in aqueous solutions. J Phys Chem 1991;95:9513–8. https://doi.org/10.1021/j100176a087.
[57] McCormick AV, Bell AT, Radke CJ. Multinuclear NMR investigation of the formation of aluminosilicate anions. J

Phys Chem 1989;93:1741–4. https://doi.org/10.1021/j100342a015.
[58] Puertas F, Martinez-Ramirez S, Alonso S, Vazquez T. Alkali-activated fly ash/slag cements: strength behaviour and hydration products. Cem. Concr. Res. 2000;30:1625–32. https://doi.org/10.1016/S0008-8846(00)00298-2.
[59] Hajimohammadi A, van Deventer JSJ. Characterisation of one-part geopolymer binders made from fly ash. Waste Biomass Valorization 2017;8:225–33. https://doi.org/10.1007/s12649-016-9582-5.
[60] Samantasinghar S, Singh SP. Effect of synthesis parameters on compressive strength of fly ash-slag blended geopolymer. Constr Build Mater 2008;170:225–34. https://doi.org/10.1016/j.conbuildmat.2018.03.026.
[61] Flanigan EM, Khatami H, Szymanski HA. Molecular sieve zeolites; advances. In: Chemistry series. vol. 101. Washington, DC: American Chemical Society; 1971. p. 201.
[62] Peng MX, Wang ZH, Shen SH, Xiao QG. Synthesis, characterization and mechanisms of one-part geopolymeric cement by calcining low-quality kaolin with alkali. Mater Struct 2005;48(3):699–708. https://doi.org/10.1617/s11527-014-0350-3.
[63] Yunsheng Z, Wei S, Zongjin L. Composition design and microstructural characterization of calcined kaolin-based geopolymer cement. Appl Clay Sci 2010;47:271–5. https://doi.org/10.1016/j.clay.2009.11.002.
[64] Sore SO, Messan A, Prud'homme E, Escadeillas G, Tsobnang F. Synthesis and characterization of geopolymer binders based on local materials from Burkina Faso-metakaolin and rice husk ash. Constr Build. Mater 2016;124:301–11. https://doi.org/10.1016/j.conbuildmat.2016.07.102.
[65] Toniolo N, Rincón A, Roether JA, Ercole P, Bernardo E, Boccaccini AR. Extensive reuse of soda-lime waste glass in fly ash-based geopolymers. Construct Build Mater 2018;188:1077–84. https://doi.org/10.1016/j.conbuildmat.2018.08.096.
[66] Lecomte I, Henrist C, Liegeois M, Maseri F, Rulmont A, Cloots R. (Micro)-structural comparison between geopolymers, alkali-activated slag cement and Portland cement. J Eur Ceram Soc 2006;26:3789–97. https://doi.org/10.1016/J.JEURCERAMSOC.2005.12.021.2006.
[67] Sathonsaowaphak A, Chindaprasirt P, Pimraksa K. Workability and strength of lignite bottom ash geopolymer mortar. J Hazard Mater 2009;168(1):44–50. https://doi.org/10.1016/j.jhazmat.2009.01.120.
[68] Yaseri S, Verki VM, Mahdikhani M. Utilization of high volume cement kiln dust and rice husk ash in the production of sustainable geopolymer. J Clean Prod 2019;250:592–602. https://doi.org/10.1016/j.jclepro.2019.05.056.

Therefore, these data indicate that OPFA can be used as an alkaline source to activate CC, obtaining geopolymers with suitable physical and thermal properties but with low mechanical properties. The use of activating solutions that use commercial alkaline silicates leads to a greater dissolution of the clay, resulting in the formation of a greater proportion of geopolymeric gel, giving alkali activated materials with better mechanical properties. In this system the type of alkali to be used in the synthesis will depend on the final objective in terms of application, obtaining better mechanical properties when potassium activating solutions are used.

Declaration of Competing Interest

The authors declare that they have no known competing financial interests or personal relationships that could have appeared to influence the work reported in this paper.

Acknowledgements

This work has been funded by the project *Development and characterization of new geopolymeric composites based on waste from the olive industry. Towards a sustainable construction* (MAT2017-88097-R), FEDER/Ministry of Science, Innovation and Universities, State Research Agency. The authors thank "Arcillas Bailen" company and Energía La Loma S.A. for supplying the clay and olive pomace fly ash, respectively. M.A. Gómez-Casero acknowledges support of MINECO (PRE2018-084073). Technical and human support provided by CICT of Universidad de Jaén (UJA, MINECO, Junta de Andalucía, FEDER) is gratefully acknowledged.

REFERENCES

[1] Catauro M, Tranquillo E, Barrino F, Dal Poggetto G, Blanco I, Cicala G, et al. Mechanical and thermal properties of fly ash-filled geopolymers. J Therm Anal Calorim 2019;138:3267–76. https://doi.org/10.1007/s10973-019-08612-y.

[2] Lee W-H, Lin K-L, Chang T-H, Ding Y-C, Cheng T-W. Sustainable development and performance evaluation of marble-waste-based geopolymer concrete. Polymers 1924;2020:12. https://doi.org/10.3390/polym12091924].

[3] Grutzeck MW, Siemer DD. Zeolites synthesised from class F fly ash and sodium aluminate slurry. J Am Ceram Soc 1997;80(9):2449–58. https://doi.org/10.1111/j.1151-2916.1997.tb03143.x.

[4] Davidovits J. Geopolymer. Chemistry and applications. 3th ed. Saint-Quentin, Francia: Institut Geopolymer; 2008.

[5] Duxson P, Fernández-Jiménez A, Provis JL, Lukey GC, Palomo A, van Deventer JSJ. Geopolymer technology: the current state of the art. J Mater Sci 2007;42(9):2917–33. https://doi.org/10.1007/s10853-006-0637-z.

[6] Nath SK. Fly ash and zinc slag blended geopolymer: immobilization of hazardous materials and development of paving blocks. J Hazard Mater 2020;387:121673. https://doi.org/10.1016/j.jhazmat.2019.121673.

[7] Ye N, Chen Y, Yang J, Liang S, Hu Y, Xiao B, et al. Co-disposal of MSWI fly ash and Bayer red mud using an one-part geopolymeric system. J Hazard Mater 2016;2016(318):70–8. https://doi.org/10.1016/j.jhazmat.2016.06.042.

[8] Autef A, Joussein E, Poulesquen A, Gasgnier G, Pronier S, Sobrados I, et al. Influence of metakaolin purities on potassium geopolymer formulation: the existence of several networks. J Colloid Interface Sci 2013;408:43–53. https://doi.org/10.1016/j.jcis.2013.07.024.

[9] Selmani S, Essaidi N, Gouny F, Bouaziz S, Joussein E, Driss A, et al. Physical-chemical characterization of Tunisian clays for the synthesis of geopolymers materials. J Afr Earth Sci 2015;103:113–20. https://doi.org/10.1016/j.jafrearsci.2014.12.009.

[10] Liew YM, Heah CY, Mohd-Mustafa AB, Kamarudin H. Structure and properties of clay-based geopolymer cements: a review. Prog Mater Sci 2016;83:595–629. https://doi.org/10.1016/j.pmatsci.2016.08.002.

[11] Seiffarth T, Hohmann M, Posern K, Ch Kaps. Effect of thermal pre-treatment conditions of common clays on the performance of clay-based geopolymeric binders. Appl Clay Sci 2013;73:35–41. https://doi.org/10.1016/j.clay.2012.09.010Get.

[12] El Hafid K, Hajjaji M. Effects of the experimental factors on the microstructure and the properties of cured alkali-activated heated clay. Appl Clay Sci 2015;116–117:202–10. https://doi.org/10.1016/j.clay.2015.03.015.

[13] Buchwald A, Hohmann M, Posern K, Brendler E. The suitability of thermally activated illite/smectite clay as raw material for geopolymer binder. Appl Clay Sci 2009;46:300–4. https://doi.org/10.1016/j.clay.2009.08.026.

[14] Bergaya F, Dion P, Alcover JF, Clinard C, Tchoubar D. TEM study of kaolinite thermal decomposition by controlled-rate thermal analysis. J Mater Sci 1996;31:5069–75. https://doi.org/10.1007/BF00355907.

[15] Hamdi N, Messaoud IB, Srasra E. Production of geopolymer binders using clay minerals and industrial wastes. Compt Rendus Chem 2019;22(2–3):220–6. https://doi.org/10.1016/j.crci.2018.11.010.

[16] Heller-Kallai L. Handbook of clay science, Development in Clay science. In: Bergaya F, Theng BKG, Lagaly G, editors. Thermally modified clay minerals. Amsterdam: Elsevier; 2006. p. 289–308.

[17] Buchwald A, Hohmann M, Posern K, Brendler E. The suitability of thermally activated illite/smectite clay as raw material for geopolymer binders. Appl Clay Sci 2009;46(3):300–4. https://doi.org/10.1016/J.CLAY.2009.08.026.

[18] Essaidi N, Samet B, Baklouti S, Rossignol S. Feasibility of producing geopolymers from two different Tunisian clays before and after calcination at various temperatures. Appl Clay Sci 2014;88–89:221–7. https://doi.org/10.1016/j.clay.2013.12.006.

[19] European Biomass Association. http://biomassmagazine.com/articles/13837/european-biomass-association-releases-2016-bioenergy-outlook. [Accessed 15 November 2020].

[20] Plan Director del olivar andaluz. Consejería de Agricultura, pesca y desarrollo rural. Junta de Andalucía. 2017. https://www.juntadeandalucia.es/export/drupaljda/Plan%20Director%20del%20Olivar.pdf. [Accessed 16 November 2020].

[21] Romero E, Quirantes M, Nogales R. Characterization of biomass ashes produced at different temperatures from olive-oil-industry and greenhouse vegetable wastes. Fuel 2017;208:1–9. https://doi.org/10.1016/j.fuel.2017.06.133.

[22] Vlyssides AG, Loizides M, Karlis PK, Clean J. Integrated strategic approach for reusing olive oil extraction by-products. J Clean Prod 2004;12:603–11. https://doi.org/10.1016/S0959-6526(03)00078-7.

[23] Roig A, Cayuela ML, Sánchez-Monedero MA. An overview on olive mil wastes and their valorisation methods. Waste

Phys Chem 1989;93:1741–4. https://doi.org/10.1021/j100342a015.
[58] Puertas F, Martinez-Ramirez S, Alonso S, Vazquez T. Alkali-activated fly ash/slag cements: strength behaviour and hydration products. Cem. Concr. Res. 2000;30:1625–32. https://doi.org/10.1016/S0008-8846(00)00298-2.
[59] Hajimohammadi A, van Deventer JSJ. Characterisation of one-part geopolymer binders made from fly ash. Waste Biomass Valorization 2017;8:225–33. https://doi.org/10.1007/s12649-016-9582-5.
[60] Samantasinghar S, Singh SP. Effect of synthesis parameters on compressive strength of fly ash-slag blended geopolymer. Constr Build Mater 2008;170:225–34. https://doi.org/10.1016/j.conbuildmat.2018.03.026.
[61] Flanigan EM, Khatami H, Szymanski HA. Molecular sieve zeolites; advances. In: Chemistry series. vol. 101. Washington, DC: American Chemical Society; 1971. p. 201.
[62] Peng MX, Wang ZH, Shen SH, Xiao QG. Synthesis, characterization and mechanisms of one-part geopolymeric cement by calcining low-quality kaolin with alkali. Mater Struct 2005;48(3):699–708. https://doi.org/10.1617/s11527-014-0350-3.
[63] Yunsheng Z, Wei S, Zongjin L. Composition design and microstructural characterization of calcined kaolin-based geopolymer cement. Appl Clay Sci 2010;47:271–5. https://doi.org/10.1016/j.clay.2009.11.002.
[64] Sore SO, Messan A, Prud'homme E, Escadeillas G, Tsobnang F. Synthesis and characterization of geopolymer binders based on local materials from Burkina Faso-metakaolin and rice husk ash. Constr Build. Mater 2016;124:301–11. https://doi.org/10.1016/j.conbuildmat.2016.07.102.
[65] Toniolo N, Rincón A, Roether JA, Ercole P, Bernardo E, Boccaccini AR. Extensive reuse of soda-lime waste glass in fly ash-based geopolymers. Construct Build Mater 2018;188:1077–84. https://doi.org/10.1016/j.conbuildmat.2018.08.096.
[66] Lecomte I, Henrist C, Liegeois M, Maseri F, Rulmont A, Cloots R. (Micro)-structural comparison between geopolymers, alkali-activated slag cement and Portland cement. J Eur Ceram Soc 2006;26:3789–97. https://doi.org/10.1016/J.JEURCERAMSOC.2005.12.021.2006.
[67] Sathonsaowaphak A, Chindaprasirt P, Pimraksa K. Workability and strength of lignite bottom ash geopolymer mortar. J Hazard Mater 2009;168(1):44–50. https://doi.org/10.1016/j.jhazmat.2009.01.120.
[68] Yaseri S, Verki VM, Mahdikhani M. Utilization of high volume cement kiln dust and rice husk ash in the production of sustainable geopolymer. J Clean Prod 2019;250:592–602. https://doi.org/10.1016/j.jclepro.2019.05.056.